Thermal lens and all optical switching study of DB dye solution

M. D. ZIDAN[1,*], A. ALLAHHAM[1], A. GHANEM[2], N. MOUSA[3]
[1]*Department of Physics, AEC, P. O. Box 6091, Damascus, Syria*
[2]*Higher Institute for Laser Research and Applications, Damascus University, Syria*
[3]*Scientific office, AEC, P. O. Box 6091, Damascus, Syria*

The thermal lens and all optical switching effects of direct blue71dye were investigated using pump-probe laser beam z-scan configuration. The results have shown the influence of the power pump laser on the temporal evolution ofa thermal lens. The thermal lens parameters have been evaluated, such as: θ, t_c, D, dn/dt, n_2 and Δn. Then, the all-optical switching process was investigated using the SXPM configuration. Our new results confirmed that the strong pump green beam can modify the probe's low laser beam by generating diffraction ring patterns, which confirms the possibility of using the direct blue71dye as nonlinear optical medium for modifying the probe laser beam signal from the "off" state to the "on" state through nonlinear optical processes. This is promising for use in light-manipulated logic circuits", which is important for practical applications.

(Received November 13, 2024; accepted June 4, 2025)

Keywords: thermal lens effect, DB71dye, All optical switching

1. Introduction

The organic dye molecules have gained much attention for their different applications in the photophysical and photochemical fields, such as nonlinear optics [1,2], solar cell systems[3], photonic devices [4], all optical switching [5], and electrochemical sensing [6]. It is well known, that organic dyes have many important features to be used as nonlinear mediums, they can absorb and emit light with a wide spectral range due to the delocalized π-electrons systems, as well as their large optical nonlinearity and fast optical response. These unique features make organic dyes ideal molecules to be used in the nonlinear optical field [7].

Different experimental techniques were utilized to study the NLO properties of organic dyes using CW or pulse regimes laser beams. These techniques are classified as, the z-scan technique [8,9], the spatial self-phase modulation (SSPM) technique [10,11], the thermal lens (TL) technique [12-14], and all optical switching (AOS) [15]. However, the TL and AOS techniques utilized the dual pump-probe z-scan configuration to study this kind of absorbing medium [16-18].

However, many articles have been reported on organic dyes to investigate their nonlinear optical properties, such as the Brilliant Green [19], acid green 5 [11], Eosin B [20], Alizarin Red S [21], Boron-dipyrromethene [22], Rose Bengal (RB) [23], Fluorescein–Rhodamine B dye mixtures [24] , and Acid Blue 29 [1,25].

Here, we report the detailed study of the thermal lens and AOS effect of an aqueous solution of direct blue71 dye (DB71). Experimental results were acquired using the pump-probe laser beam z-scan technique. The thermal lens parameters of the DB71dye were deduced in addition to some results related to AOS effect. This study will lead to creating a deep understanding of the behaviors of the DB71 dye as well as a way of further development of optical devices, which are based on organic dyes.

2. Experimental techniques

2.1. Samples preparation

The DB71dye was purchased from Sigma-Aldrich and it was used without any processes, and then it was dissolved in deionized water with a concentration of 2×10^{-4} *M*. Fig. 1 shows the molecular structure of DB71 dye. The UV-Vis absorption spectrum of the DB71dye dissolved in water was shown in Fig. 2 (using UV-1601PC Shimadzu spectrophotometer). The spectrum exhibits a strong absorption band with a maximum wavelength located around λ=590 nm due to π-π* electronic transitions.

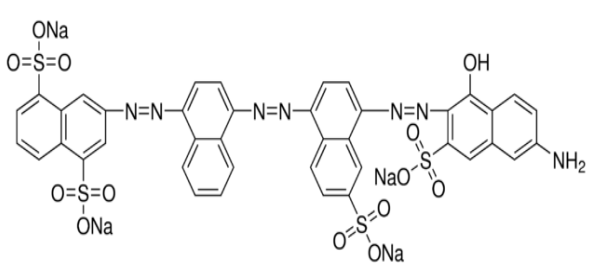

Fig. 1. Molecular structure of DB71 dye

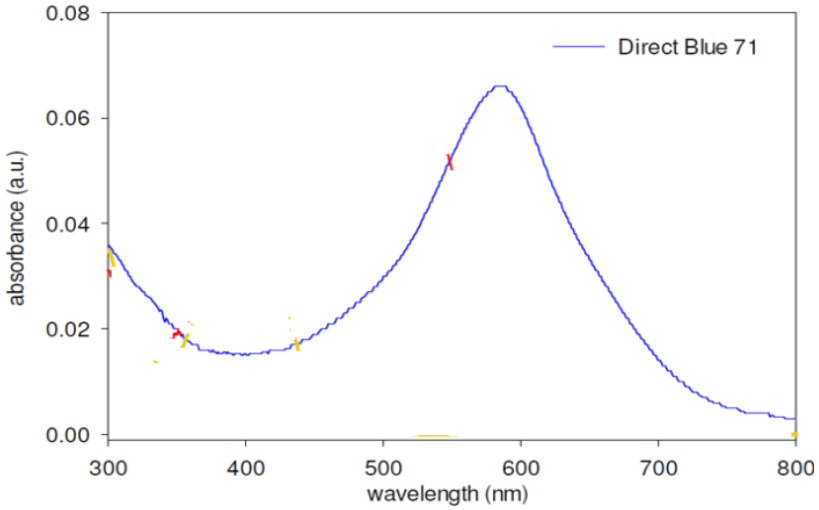

Fig. 2. UV-Vis absorption spectrum of DB71dye dissolved in deionized water with concentration of 2×10^{-4} M (colour online)

2.2. Thermal lens experimental setups

Experimental thermal lens data was obtained using a typical dual beam pump-probe z-scan method, which is similar to the experimental setup, mentioned in our previous work [26]. We present brief details of the used setup. A continuous laser beam (λ=532nm, laser diode, Gaussian TEM00 beam) as an excited pump beam, and a low-power probe laser beam (λ=635nm laser diode, Gaussian TEM00 beam) with power of 1 mW were directed to a 2 mm quartz cell containing the DB71solution. Then, the laser transmittance signals during thermal lens formation were detected by a silicon photo-detector, which was connected to a digital Tektronix oscilloscope to track the formation of the thermal lens in the nonlinear medium (DB71 dye). Adjustment of the pumped laser beam was performed using a pulses generator to obtain the exposure period to achieve the "on/off" status.

2.3. All optical switching experimental setups

The experimental data for the DB71dye was obtained using the similar scheme mentioned in our previously reported work [15,27]. Again, we give a very brief to illustrate the effect of all optical switching, when the pumping laser beam (green beam, λ=532nm) and the low-energy probe laser beam (red beam, λ=635nm) are combined in a 2 mm quartz cell filled with DB71dye, the patterns of the diffraction rings of the green laser beam and the red laser beam appear as circular rings. Both green and red diffraction ring patterns were observed on a screen that was about 100 cm behind the cell. Next, a digital camera was used to take pictures of the red and green diffraction rings. The experiment setup was based on SXPM configuration. The two laser beams were guided by the positive lens (f=10 cm) and monitored by two silicone photodiode PD1 and PD2 detectors (Thorlab, DET-110), which were connected to a digital oscilloscope (Tektronix TDS 3054B). The pulse generator was utilized to control the green pumping laser beam to get the desired frequency.

3. Results and discussion

3.1. Thermal lens study

The thermal lens effect of DB71 dye solution (with a concentration of 2×10^{-4} *M*) was studied using the double beam z-scanning technique (SXPM configuration), where a continuous laser diode with λ = 532nm as excitation beam was used and at the same time a red diode laser was used as a probe laser with a λ = 635nm. Fig. 3 shows the experimental results for the study of thermal lens signals at two laser pumping powers, P=10 and 25 mW. The recorded thermal lens signals decrease with increasing pumping powers (P), and a decrease in time values (T_C) occurs, which corresponds the previous reported work in the literature[28, 29]. Also, the solid lines indicate to the results of the fitting processes of experimental data using the numerical integration of the theoretical thermal lens equation (1) [30]:

$$S(t)=\frac{I(t)}{I(0)}=\left[1-\frac{i\theta}{4}\left[-\left(\frac{P_E{}^2}{2}\frac{(1+iV\_2m)^2}{2m(1+V)}\right)\left\{2i\tan^{-1}\left\{\frac{2mV}{\left[\left(1+2m\right)^2\right)+V^2\right]\left(\frac{t_c}{2t}\right)+1+2m+v^2}\right\}+\ln\left\{\frac{\left[1+\frac{2m}{\left(1+\frac{2t}{t_c}\right)}\right]^2+V^2}{(1+2m)^2+V^2}\right\}\right\}-P_E^2\left[\frac{2m}{(1+iV)}\ln\left(1+\frac{2t}{t_c}\right)+\left(\frac{\frac{2t}{t_c}}{1+\frac{2t}{t_c}}\right)\right]\right]\right]^2 \quad (1)$$

The parameters in equation 1 are defined as:
$\upsilon = (z/z_p)$, where z is the distance of the sample from the beam waist position of probe beam and z_p is Rayleigh range of probe beam, $m= (\omega_p/\omega_e)^2$, where ω_p and ω_e are the beam waists of the probe and the pump beams at the sample position.

The thermal diffusion time:

$$t_c = \left(\frac{\omega_e{}^2}{4D}\right) \quad (2)$$

where D is the thermal diffusivity.

Also, the on-axis phase shift (θ) is:

$$\theta = \frac{\alpha P_e L}{k \lambda_p}\left(\frac{d n}{d T}\right) \quad (3)$$

where p_e is the pump laser power, λ_p is the wavelength of the probe beam, α is the linear absorption coefficient, L is the sample thickness, dn/dT is the thermo-optic coefficient, and k is the thermal conductivity of the solvent.

The Peclet number (P_E) presents the following rate [30]:

$$P_E = \frac{rate\ of\ convection}{rate\ of\ conduction} = \frac{\omega_e v_x}{4D} \quad (4)$$

The results also showed that the DB71 dye solution has the behavior of a self-defocusing medium due to the formation of a negative thermal lens[27]. As a result of creating the thermal lens, the intensity of the transmitted laser beam was reduced, and over time, the final stable state is reached. Thus, the thermal lens effect signal is reduced before reaching the steady state. How much thermal lens signals were reduced, depends on the rate of thermal heating convection part. The geometrical values of m=32.52 and V=10.61 were calculated using constant geometrical experimental parameters, which were used in the process of fitting experimental data. Based on the fitting processes, all the calculated parameters obtained D, v_x, T_C, P_E and θ were listed in Table 1 for the results of the DB71 dye solution. Also, it can be said that our experimental data correspond to the results of the theoretical thermal lens model used in the reference [30]. It can be said that the correlation factor between fitting and exp data is almost over %90.

Table 1. Summarizes thermal lens parameters t_c, v_x, D, θ and P_E (m=32.52 and V=10.61)

Power (mW)	t_c (s) $\times 10^{-2}$	P_E	θ	v_x(cm/s) $\times 10^{-2}$	D(cm^2/s) $\times 10^{-5}$
10	21.36	0.52	1.14	8.85	4.65
25	8.00	0.48	1.23	20.00	12.20

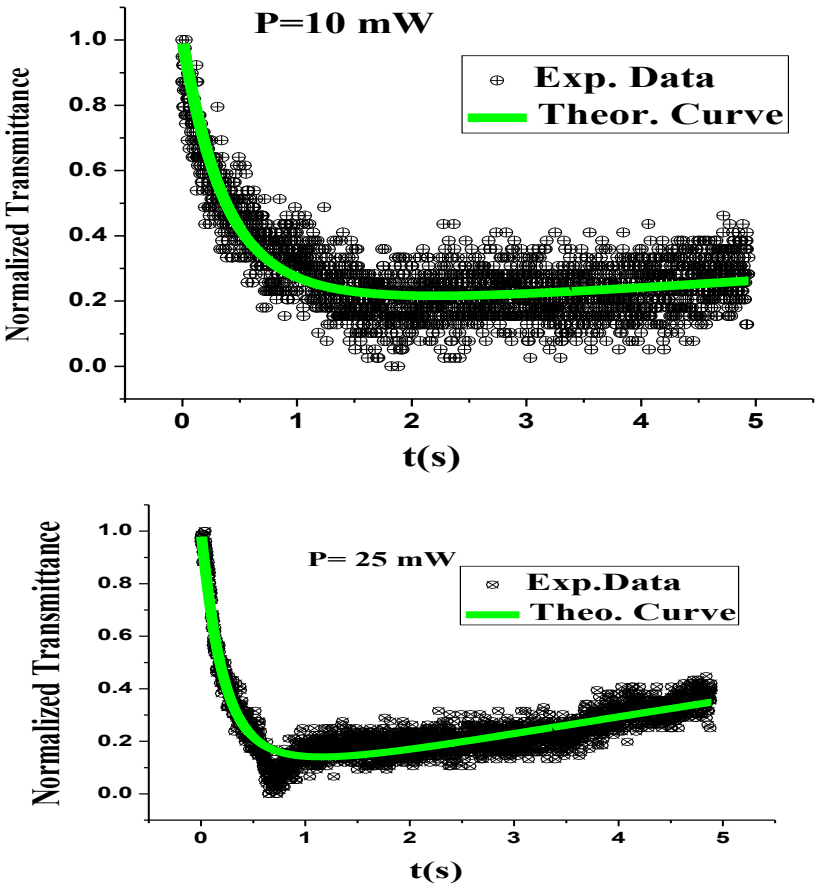

Fig. 3. Time dependence of thermal lens signals of DB71 dye with a concentration of 2×10^{-4} M at laser pumping powers of 10 and 25 mW (the symbols). Solid lines refer to the results of the experimental data fitting processes (colour online)

3.2. All-optical switching study

The all-optical switching effect was studied using a continuous red laser beam (λ=635nm) controlled by a continuous green laser beam (λ=532nm). Fig. 4 shows the observed red and green diffraction ring patterns. The power of the red laser beam was set at 1 mW, while the power of the green laser beam was gradually increased, starting from 50, 75 and 100 mW. The pulse generator was operated to control the firing time of the green laser beam. At first, when t = 0, there is no radiation of green laser light, only a small red-light spot can be observed, and no spatial self-modulation effect was observed with the 1 mW red laser beam. Then, by applying higher power such as 50 mW of green laser to be sent onto the NL medium cell (DB71 dye|), and a clear change in the shape of the red laser spot was detected, a new diffraction ring pattern was recognized. In addition, to the red diffraction rings, also green diffraction rings were observed behind the sample at the far field on the white screen. As the power of the green laser increased, there was an increase in the absorption rate of green laser photons (laser energy) by the molecules of DB71dye and this leads to a higher level of nonlinear in the DB71 dye solution. The resulting red and green diffraction ring patterns were then expanded in proportion to the increasing powers of the green laser, in the order of 50, 75 and 100 mW. It can be seen that the number of rings and their sizes of both red and green laser light increased with increasing the powers of the green laser. In addition, the brightness and width of the diffraction ring gradually decrease towards the center. However, it can be said that the complete AOS effect was achieved using the DB71 dye solution. As, the red laser beam passes through the DB71 solution, the change of refractive presumption (Δn_2) of the laser light increased by the green laser light will also cause a changing of the phase shift of the red laser light and it will be deflected and concentric diffraction rings are formed.

The diffraction rings look like asymmetry (distortion) which means that the part of the thermal convection has contributed to the distortion (squeezing) process [31]. Also, by analyzing the diffraction rings of both laser radiations (Fig. 4), there is a linear relationship between the number of diffraction rings (red/green diffraction ring patterns) and the increasing powers of the green laser, as shown in Fig. 5.

The nonlinear refractive index (n_2) of the DB71 dye solution can be calculated using equation 5 [32].

$$n_2 = \frac{\pi \omega_o^2 \lambda}{2L_{eff}} \frac{N}{p} \quad (5)$$

The slope (N/P) was extracted using the data in Fig. 5. The experimental values of α_0, Slope (N/P), beam waist (w_0) and n_2 are tabulated in Table 2.

Table 2. Summarizes the parameters of α_0, (N/P), w_0, and n_2 at λ=532 nm using DB71 dye solution with concentration of 2×10^{-4}M

Laser wavelength	Linear absorption coefficient α_0 (cm^{-1})	Slope (N/P)	Beam waist w_0 (cm)	n_2 (cm^2/w)
λ= 532nm	18.46	0.04	62.5×10^{-4}	2.6×10^{-9}

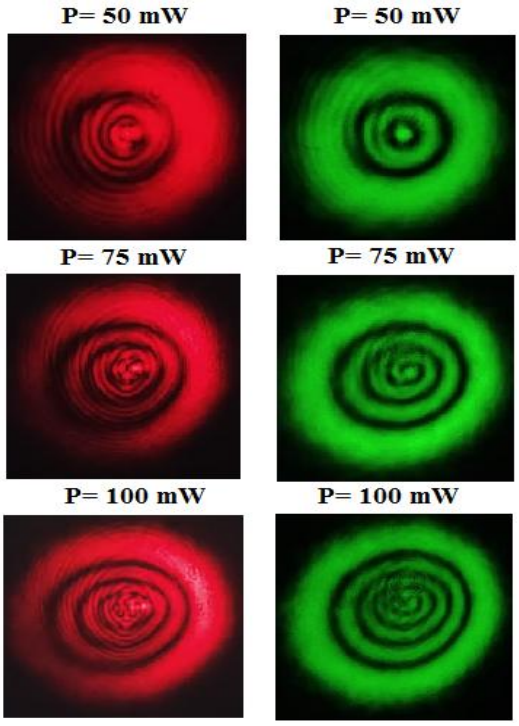

Fig. 4. Images of diffraction ring patterns for red laser light (635nm) and green laser light (532nm) at 50, 75 and 100 mW, using DB71 dye with concentration of 2×10^{-4}M (colour online)

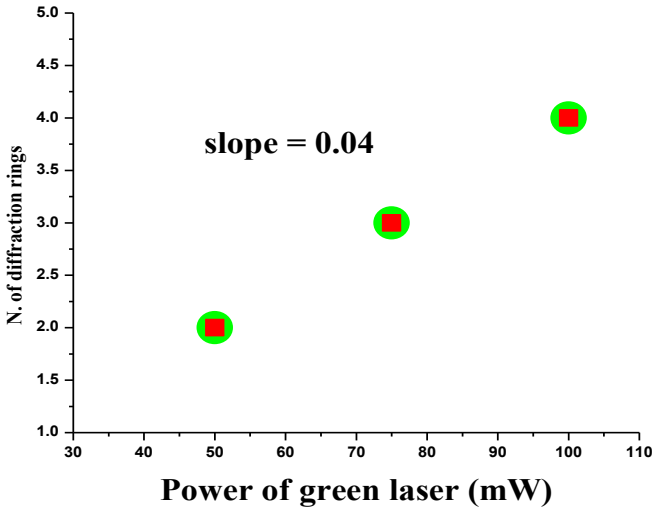

Fig. 5. Number of red and green ring patterns applying different powers of green laser of DB71 dye solution with concentration of 2×10^{-4}M (colour online)

To study the behavior of the AOS time response, two silicon photodiode detectors (PD1) and (PD2) were installed in front of the transmitted green and the red probe laser beams, and both of the detectors were connected to a digital oscilloscope, and it is assumed that both detectors record the two signals to monitor the effects of AOS. As mentioned earlier, the pulse generator was used to control the firing of CW green laser beam. When the green laser beam (λ=532nm) was stopped, the red laser beam (λ=635nm) was not deflected. Then, when the green laser light was turned on, the diffraction rings of the red laser light were reconfigured and the transmittance signals could be recorded using the PD2 detector. The variation data of the transmittance signals during the green laser light on and off were displayed as shown in Fig. 6. The transmittance signals were recorded during the operation of the green laser light at three frequencies 1 and 10 Hz, where the pumping laser power was fixed at 30 mW and a probe laser of at 1 mW. The signal curves were recorded in the red laser light (bottom) and the modified green laser light (top) representing the AOS process of the DB71 dye solution with a concentration of 2×10^{-4}M.

As the green laser signal passes through the DB71 dye solution, the output intensity of the red laser beam decreases, which was expressed as the off state due to the formation of a thermal lens inside the NL medium (DB71 dye solution) [33]. As the green laser beam is turned off, the red laser beam produced increases. Switching times were seen in the microsecond domain. Cycles were repeated according to the applied frequency value. It has been observed that the time response to AOS process becomes very short with increasing frequency value on the pumping laser (Fig. 6). This means that the frequency value of the green laser beam increases, the intensity of the weak red laser beam decreases and also the time width decreases [34].

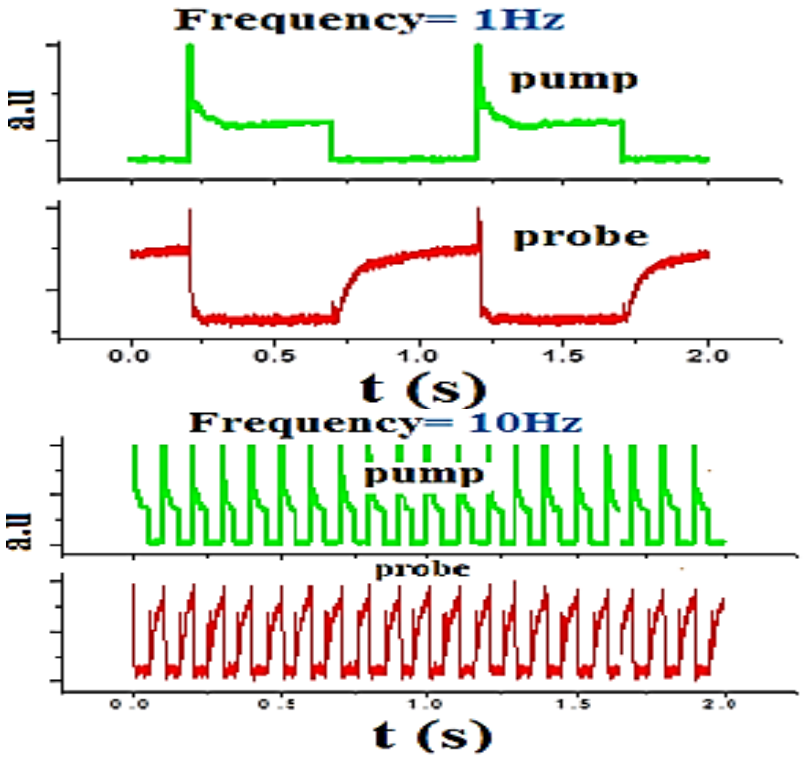

Fig. 6. AOS effect: pump beam (upper curve) and probe beam (bottom curve), at frequencies of 1 and 10 Hz, pumping laser power 30 mW using DB71 dye solution at a concentration of 2×10^{-4} M (colour online)

4. Conclusion

We observed the thermal lens effect using the pump-probe z-scan configuration using DB71 dye solution. The thermal lens linearly increased with pumped laser powers. The effect of the pump laser power on the probe beam shape and its quality was observed. The results have indicated that the thermal lens effect parameters: t_c, v_x, D, θ and PE, increase with the pump laser power as a result of deforms the phase shift of the probe beam profile.

The transit signal curves of strong laser and low laser power have been observed; the green laser was fired at a frequency of 1 and 10 Hz at a power of 30 mW to find the suitable time response of the AOS effect. The frequency of firing the green laser has a large influence on the time width of the optical time response.

Acknowledgements

We would like to thank the AEC of Syria for the financial support. Also, A. Ghanem would like to thank Damascus University.

References

[1] A. Ghanem, M. D. Zidan, M. S. El-Daher, Results in Optics **9**, 100268 (2022).
[2] H. Motiei, A. Jafari, R. Naderali, Optics and Laser Technology **88**, 68 (2017).
[3] V. Jeux, O. Segut, D. Demeter, T. Rousseau, M. Allain, C. Dalinot, L. Sanguinet, P. Leriche, J. Roncali, Dyes and Pigments **113**, 402 (2015).
[4] J. Hwang, E. Hinds, New Journal of Physics **13**, 085009 (2011).
[5] B. Atorf, H. Mühlenbernd, T. Zentgraf, H. Kitzerow, Optics Express **28**, 8898 (2020).
[6] R. Yahya, A. Shah, T. Kokab, N. Ullah, M. K. Hakeem, M. Hayat, A. Haleem, I. Shah, ACS Omega **7**, 34154 (2022).
[7] S. M. Shavakandi, S. Sharifi, J. Optoelectron. Adv. M. **19**(9-10), 604 (2017).
[8] S. Jeyaram, T. Geethakrishnan, Journal of Fluorescence **30**, 1161 (2020).
[9] S. Zongo, K. Sanusi, J. Britton, P. Mthunzi, T. Nyokong, M. Maaza, B. Sahraoui, Optical Materials **46**, 270 (2015).
[10] F. Mostaghni, Y. Abed, Materials Science **36**, 445 (2018).
[11] Q. M. A. Hassan, Optics and Laser Technology **106**, 366 (2018).
[12] S. Salmani, M. H. M. Ara, Optics and Laser Technology **82**, 34 (2016).
[13] H. A. Badran, Applied Physics B **119**, 319 (2015).
[14] A. Marcano, C. Loper, N. Melikechi, Journal of the Optical Society of America B **19**, 119 (2002).
[15] M. D. Zidan, A. Allahham, A. Ghanem, N. Mousa, B. Abdallah, A. A. Salman, Journal of Nonlinear Optical Physics and Materials **34** ,9(2025).
[16] M. D. Zidan, M. M. Al-Ktaifani, M. S. El-Daher, A. Allahham, A. Ghanem, Optoelectronics Letters **17**, 183 (2021).
[17] G. Boudebs, Materials **14**, 5533 (2021).
[18] M. Franko, C. D. Tran, Encyclopedia of Analytical Chemistry, John Wiley & Sons, Ltd., 2010.
[19] R. K. Choubey, S. Medhekar, R. Kumar, S. Mukherjee, S. Kumar, Journal of Materials Science: Materials in Electronics **25**, 1410 (2014).
[20] N. Karimi, S. Sharifi, S.S. Parhizgar, S. M. Elahi, Optical and Quantum Electronics **50**, 209 (2018).
[21] S. A. Sangsefedi, S. Sharifi, H. R. M. Rezaion, A. Azarpour, Journal of Fluorescence **28**, 815 (2018).
[22] P. Aloukos, I. Orfanos, I. Dalamaras, A. Kaloudi-Chantzea, A. Avramopoulos, G. Pistolis, S. Couris, Materials Chemistry and Physics **283**, 126057 (2022).
[23] T. S. Kondratenko, T. A. Chevychelova, O. V. Ovchinnikov, M. S. Smirnov, A. I. Zvyagin, Journal of Russian Laser Research **44**, 179 (2023).
[24] A. Kurian, S. D. George, V. P. N. Nampoori, C. P. G. Vallabhan, Spectrochimica Acta Part A: Molecular and Biomolecular Spectroscopy **61**, 2799 (2005).
[25] A. Ghanem, M. D. Zidan, M. S. El-Daher, A. Allahham, Optik **252**, 168499 (2022).
[26] M. D. Zidan, A. Allahham, A. Ghanem, N. Mousa, B. Abdallah, A. Al Salman, Results in Optics **16**, 100692 (2024).
[27] M. D. Zidan, A. W. Allaf, A. Allaham, A. AL-Zier, Optik **283**, 170939 (2023).
[28] M. D. Zidan, A. Arfan, M. S. El-Daher, A. Allahham, A. Ghanem, D. Naima, Optical Materials **117**, 111133 (2021).
[29] S. Singhal, D. Goswami, ACS Omega **4**, 1889 (2019).
[30] S. Singhal, D. Goswami, Analyst **145**, 929 (2020).
[31] T. Neupane, B. Tabibi, W.-J. Kim, F.J. Seo, Crystals **13**, 271 (2023).
[32] T. Thomas, K. V. Jayaprasad, K. R. Vijesh, V. P. N. Nampoori, M. Vaishakh, Journal of Optics **25**, 115401 (2023).
[33] H. A. Badran, R. C. Abul-Hail, H. S. Shaker, A. I. Musa, Q. M. A. Hassan, Applied Physics B **123**, 31 (2016).
[34] T. Xu, G. Chen, C. Zhang, Z. Hao, X. Xu, J. Tian, Optical Materials **30**, 1349 (2008).

*Corresponding author: pscientific8@aec.org.sy